Available online at www.sciencedirect.com
SCIENCE DIRECT®
Journal of Physics and Chemistry of Solids 66 (2005) 1274–1280
JOURNAL OF PHYSICS AND CHEMISTRY OF SOLIDS
www.elsevier.com/locate/jpcs

Conduction behaviour and thermoelectric power of Ag_x $(As_{0.4}Se_{0.6})_{100-x}$ chalcogenide system

A.M. Ahmed*, N.M. Megahid, M.M. Wakkad, A.K. Diab

Physics Department, Faculty of Science, South Valley University, 82524 Sohag, Egypt

Received 4 October 2004; revised 1 March 2005; accepted 25 March 2005

Abstract

Chalcogenide bulk alloys of Ag_x $(As_{0.4}Se_{0.6})_{100-x}$ ($x=5$, 7.5, 10, 12.5, 15 and 17.5) system were prepared by the conventional melt-quench technique. The d.c. electrical conductivity (σ) and thermoelectric power (TEP) measurements were carried out in the temperature range from 83 to 373 K and from 253 to 373 K, respectively. Variations of both σ and TEP with ambient temperature proved the p-type semiconducting behaviour of these materials. The current density-electric field characteristics were found to be linear. The activation energies, calculated from both the electrical conductivity E_σ and thermoelectric power E_s, were found to be dependent on composition.

PACS: 61.43.Dq; 66.10.Ed; 72.15.Cz; 72.15.Jf

Keywords: $Ag_x(As_{0.4}Se_{0.6})_{100-x}$; XRD; D. Electrical conductivity; Ionic conductivity; Activation energy; Mott parameters; Seebeck coefficient

1. Introduction

Many approaches have been proposed to explain the compositional dependence of various physical properties of chalcogenide network glasses [1–5]. One of these approaches is the so-called chemically ordered network model (CONM) [1], in which the formation of heteropolar bonds is favored over the formation of homopolar bonds. In this model, the glass structure is assumed to be composed of cross-linked structural units of the stable chemical compounds (heteropolar bonds) of the system and excess, if any, of the elements (homopolar bonds). Due to chemical ordering features such as extremum, a change in slope or kink occur for the various properties at the so-called tie line or stoichiometric compositions [6]. At these compositions the glass structure is made up of cross-linked structural units consisting of heteropolar bonds only.

Itoh [7] has investigated the X-ray diffraction, X-ray photoelectron spectroscopy and optical properties of Ag_x $(Cu_x)(As_{0.4}Se_{0.6})_{100-x}$ ($0 \leq x \leq 35$ at%). His results could be summarized briefly as follows: (a) the band gap energies (E_g) of Ag(Cu)–As–Se system were decreased with increasing Ag (Cu) content, in which Ag–As–Se glasses possess larger band-gap energies than Cu–As–Se glasses at the same Ag (Cu) content. (b) Ag and Cu addition induce Ag 4d and Cu 3d bands near the top of the valence band, where the energy of Cu 3d band is larger than that of Ag 4d band. (c) The localized-state distributions of the Ag-containing system exhibit T_u (the characteristic temperature in the Urbach tail) and T_o (the characteristic temperature of localized-state distribution) slightly larger than those in g-As_2Se_3. In contrast, the Cu-containing system has Tu and T_o values larger than those of g-As_2Se_3.

Therefore, the band structure of Ag (Cu)–As–Se glasses was considered as following: according to structural studies on local environments around Ag and Cu atoms in Ag (Cu)–As–Se glasses [8,9] Ag and Cu atoms are bounded to Se atoms with coordination number of 2 and 4, respectively. In addition, Itoh's X-ray photoelectron spectral data has revealed that the Ag 4d and Cu 3d bands are close in energy to the Se up band constituting the top of the valance band in As-Se glasses. Hence, the d band will interact with the Se up band forming d-p anti-bonding states in the upper valance region. Hence, with increasing in Ag (Cu) content Itoh has recognized that the top of

* Corresponding author. Tel.: +20 936 029 64; fax: +20 936 019 50.
E-mail address: fikry_99@yahoo.com (A.M. Ahmed).

0022-3697/$ - see front matter © 2005 Elsevier Ltd. All rights reserved.
doi:10.1016/j.jpcs.2005.03.007

the valance band would shift upward and consequently the band-gap energy decrease. Moreover, since the d-p hybridization effect will become stronger when the d band is much close to the Se-4p band, the upper shift of the top of the valence band will be greater when Cu is added. Thence, Cu–As–Se glasses exhibit a distinctly smaller E_g than do Ag–As–Se glasses. In this consideration, Itoh has implicitly assumed that bottoms of conduction bands in Ag (Cu)–As–Se glasses also consist of As–Se anti-bonding states.

Solid state ionic materials are of great interest due to their potential applications in electrochemical devices like batteries, fuel cells, sensors, electrochromic devices etc. [10–12]. For this we studied the conduction behaviour and thermoelectric power of the glassy Ag_x $(As_{0.4}Se_{0.6})_{100-x}$ compositions. The conduction behaviour and the electrical parameters were identified from the electrical conductivity measurements. The kind of charge as well as the activation energy of TEP were determined from the thermoelectric power measurements. A special attention paid to the investigated alloys as thermoelectric energy converts, especially in bulk form.

2. Experimental techniques

The considered Ag_x $(As_{0.4}Se_{0.6})_{100\_x}$ alloys were prepared through two steps using appropriate amounts of pure Ag, As and Se (Aldrish with purity grade 99.999%). Firstly, the binary As_2Se_3 alloy was prepared by the usual melt quench technique. The required weights of the elements As and Se were charged into silica tube with 1 cm diameter and 20 cm length. The tube was sealed after evacuation up to 10^{-5} Torr. Then it was heated at 1173 K for 7 h, during which the tube was shaken several times to ensure good mixing of the constituents. The tube was suddenly quenched in iced water. In the second step, the appropriate weights of Ag and As_2Se_3 were mixed and charged into cleaned silica tubes, then heated at 1300 K for 24 h. Finally, the charged tubes were suddenly quenched in iced water. Bulk samples with parallel and optically flat surfaces were prepared by sawing.

The measurements of the d.c. electrical conductivity and current–voltage characteristics were carried out using a pressure contact sample holder. The adjacent parallel surfaces of sample were pointed with silver paste as contact electrodes. A conventional series current circuit was used. The current was measured by using electrometer type Keithley model 610 C (sensitivity 10^{-15} A), while the potential difference was measured by means of Keithley 175 μV (sensitivity 1 μV). A Copper-Constantan junction thermocouple was used for monitoring the temperature. The thermoelectric power measurements were carried out using a differential temperature sample holder ended with two graphite electrodes. The difference in temperature between the two opposite surfaces of the sample was equal to 3 °C during the whole measurements. The thermoelectric power (TEP) voltage was measured by using Hewlett Packard 34401 A multimeter (sensitivity 1 μV).

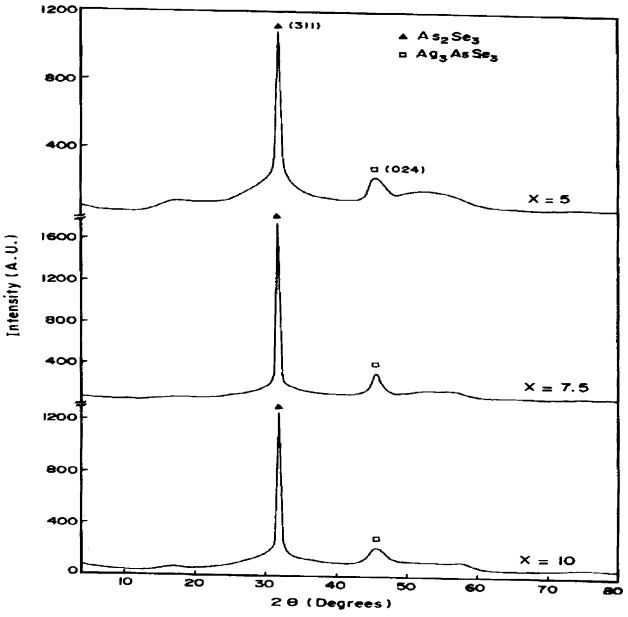

Fig. 1. X-ray diffraction patterns for $Ag_x(As_{0.4}Se_{0.6})_{100\_x}$ (x=5, 7.5 and 10 at%.) bulk materials.

3. Results and discussion

The X-ray diffraction was used to study the effect of silver content on the crystallization structure of the investigated materials. Fig. 1 shows the X-ray diffractograms of the as-prepared Ag_x $(As_{0.4}Se_{0.6})_{100\_x}$ compositions with x=5,7.5 and 10 at%. The diffractograms

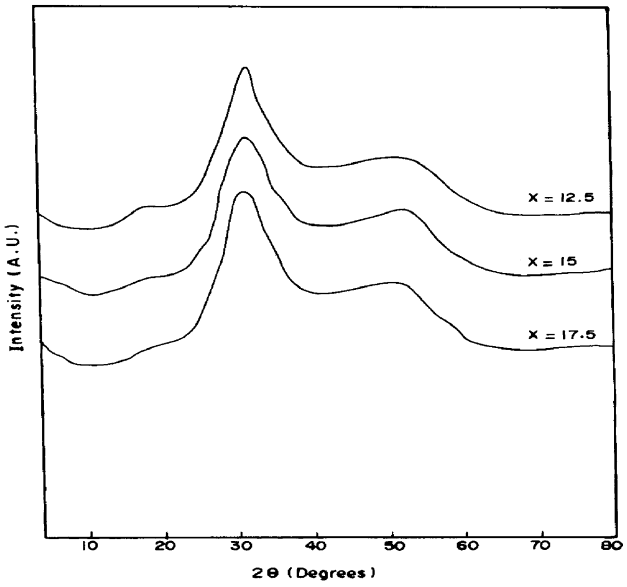

Fig. 2. X-ray diffraction patterns for $Ag_x(As_{0.4}Se_{0.6})_{100\_x}$ (x=12.5, 15 and 17.5 at%.) bulk materials.

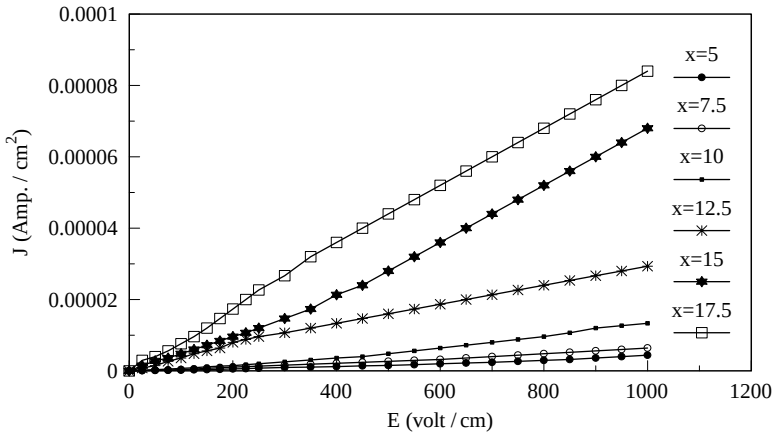

Fig. 3. The relation between the current density (J) and the electric field (E), measured at room temperature, for compositions.

possess two characterizing peaks, one for the preferred (311) plane of the crystalline As_2Se_3 phase and the other for (024) plane of the crystalline Ag_3AsSe_3 phase. On contrary the diffractograms of the compositions prepared with $x=12.5$, 15 and 17.5 at% emphasize the amorphous nature as shown in Fig. 2. Three halo peaks appear in the patterns. The first diffraction peak (FDP) located at $2\theta\sim17°$, which arises from medium-range structural order [13]. The second ($2\theta\sim30°$) and the third ($2\theta\sim52°$) halo peaks are mainly results from the correlation between the second nearest neighbors and between the nearest neighbors [14]. With increasing Ag content the FDP weakens, and almost disappears at $x=15$ at%. In addition, the second and third halo peaks shift to lower angles with increasing in Ag content. However, it may be noted that these latter observations are in good agreement with those previously obtained by Itoh [7].

The current density (J)-electric field (E) characteristics of as-prepared bulk specimens of the Ag_x $(As_{0.4}Se_{0.6})_{100\_x}$ chalcogenide system with $5\leq x\leq17.5$ at% were investigated at different temperatures (T) equal to 83, 153, 203, 300, 333, 353 and 373 K. Fig. 3 shows the J (A cm^{-2}) versus E (V cm^{-1}) plots measured at room temperature (300 K) for as-prepared compositions. It is seen that the general feature of the J–E characteristics is a linear shape within most of the range of the applied electric field. Moreover, the J–E plots discriminated upward in a regular manner proving sequential dependence of the electrical conductivity on the Ag content. Besides, we have observed that, the values of J confused in the low range of E.

Figs. 4 and 5 show, respectively (for instance), the J–E characteristics of the as-prepared specimens of the investigated system with $x=5$, and 15 at%. The measurements were carried out at different temperatures. These figures reveal that the J–E characteristics are nearly linear. J increases with increasing temperature, a matter confirms a temperature enhancement of the electrical conductivity. On the other hand, the effect of the applied electric field is more pronounced especially in its relatively higher range. The above findings indicate that the electrical conductivity can be enhanced by both the temperature and the electric field, and the role of T is more pronounced at higher values of E.

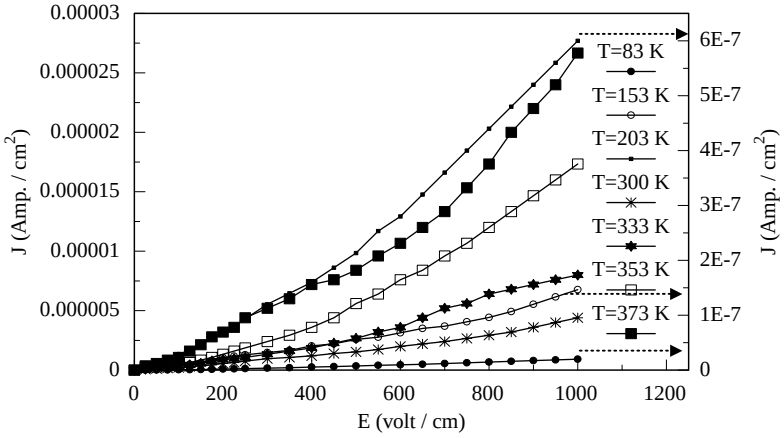

Fig. 4. J–E characteristics, measured at different ambient temperatures, for $Ag_5(As_{0.4}Se_{0.6})_{95}$ composition.

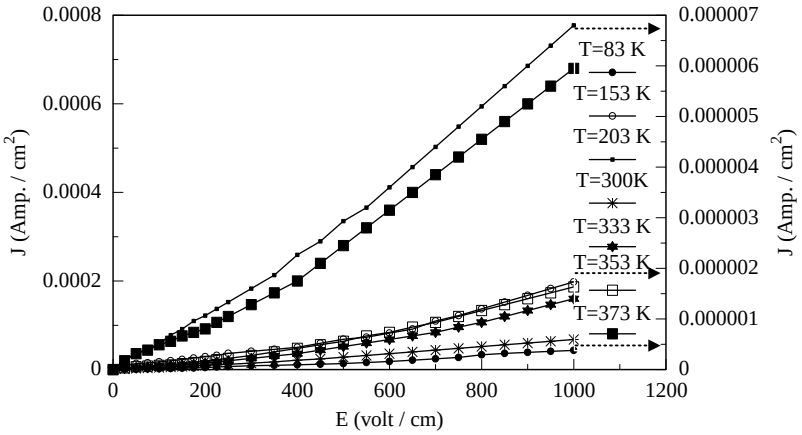

Fig. 5. *J–E* characteristics, measured at different ambient temperatures, for $Ag_{15}(As_{0.4}Se_{0.6})_{85}$ composition.

Regarding to the different corresponding *J–E* characteristics, the following conclusions, can be drawn.

(i) The general feature is that of ohmic contact (linear characteristics) for the most range of *E*.
(ii) The electrical conductivity shows field dependence especially at the relatively higher field range.

For the six compositions, the double logarithmic relation between *J* and *E*, measured at different temperatures, are linear possessing one stage with its own slope. Plots of LnJ versus LnE, however, suggest a power law, describing the dependence of *J*(*E*) which can be formulated empirically as follows:

$$J = CE^n \tag{1}$$

The values of *n* were calculated for all the compositions at considered temperature. It is found that the value of the exponent *n* is about 1 for all samples and temperatures.

The variation d.c. electrical conductivity with the ambient temperatures in the range of 83–373 K, for the investigated Ag_x $(As_{0.4}Se_{0.6})_{100\_x}$ (where $5 \leq x \leq 17.5$ at%) compositions, is shown in Fig. 6. It is seen that σ increases with increasing *T* for all compositions. Hence, the investigated compositions behave as a semiconducting material. These results indicate that, at any given temperature the d.c. conductivity increases with increasing Ag content, a matter that can be attributed to its ionic nature. Accordingly [15], the ionic conduction of Ag is larger than its electronic conduction. However, the valance band structures indicates different nature of Ag–Se bonds in Ag–As–Se systems. That is because of the energies of the Ag 4d orbital are lower than those of Se 4p orbital, wavefunctions of the d orbitals do not spread extensively towards the Se atoms. Hence, overlap of the 4d orbitals with 4p orbitals is considered to be small and accordingly, the Ag–Se bonds are expected to have strong ionic nature. Besides, the increase of Ag content enhanced the conductivity of Ag-chalcogenide glasses because their band-gap energies decreases with increasing the former [7]. Regarding again to the plots of Ln σ versus 1000/*T* shown in Fig. 6, it can be concluded that the conduction phenomena of the investigated glasses is proceeded through the following two distinct conduction channels:

(i) At relatively higher range of temperature ($T > 233$ K) the conductivity is strongly dependente on *T*. This represents the conduction through the extended states. In this case, the dependence of σ on *T* can be represented by the well-known Arrhenius formula:

$$\sigma = \frac{\sigma_o'}{T}\exp(-E_\sigma/k_B T) \tag{2}$$

were σ_o' is the pre-exponential factor (which includes the carrier mobility and density of states), E_σ is the corresponding activation energy of electrical conductivity (which is a function of the electronic energy levels of the chemical interacting atoms in the glass) and k_B is the Boltzmann's constant. Data shown in Fig. 7 depicts the σT versus $1/T$ dependence for the compositions

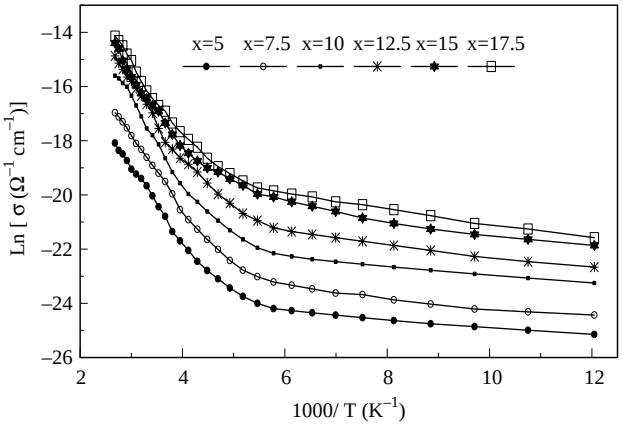

Fig. 6. The temperature dependence of the electrical conductivity for $Ag_x(As_{0.4}Se_{0.6})_{100\_x}$ compositions.

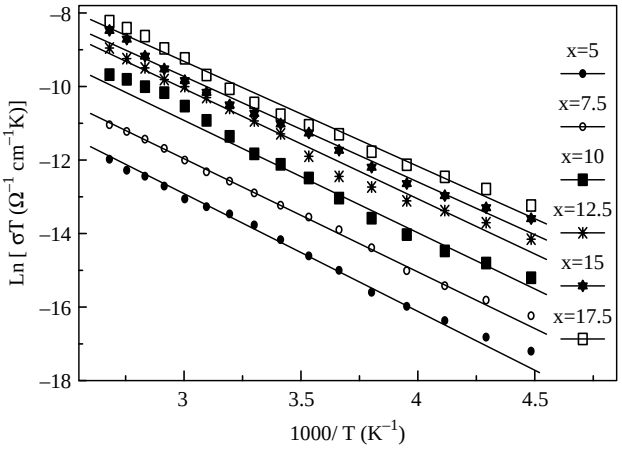

Fig. 7. Plots of Ln(σT) versus 1000/T for $Ag_x(As_{0.4}Se_{0.6})_{100\_x}$ compositions.

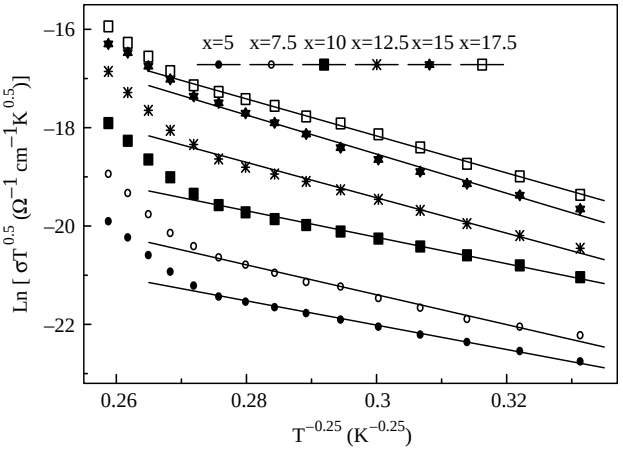

Fig. 8. Plots of (Ln σ $T^{0.5}$) versus $T^{-0.25}$ for $Ag_x(As_{0.4}Se_{0.6})_{100\_x}$ compositions.

investigated. Linear fitting of the data shown in Fig. 7 gives us the values of both E_σ and σ'_o, for the investigated compositions, which are summarized in Table 1.

The continuous decrease of E_σ with increasing Ag ratio is in good agreement with those obtained by other authors [7,16]. They attributed the observed results to the electronic structure of the Ag_x $(As_{0.4}Se_{0.6})$ $_{100\_x}$ compositions as mentioned before. Additionally, the values of σ'_o increase with increasing Ag content.

(ii) the conductivity data in the low temperature region ($T \leq 223$ K) shows that, σ is slightly dependent on temperature, which is the behaviour of conduction through localized states. In this case the dependence of conductivity on temperature can be described according to Mott's formula [17] for variable-range hopping (VRH) conduction. In Mott's theory the temperature dependent conductivity can be accounted for in terms of:

$$\sigma\sqrt{T} = \sigma''_o \exp(-B/T^{1/4}) \tag{3}$$

with

$$B = T_o^{1/4} = 1.66[\alpha^3/k_B N(E_F)]^{1/4} \tag{4}$$

where σ''_o is a pre-exponential factor, α is the coefficient of exponential decay of the localized state wavefunction, which assumed to be 0.124 $Å^{-1}$ [18] and N (E_f) is the density of localized states (DOLS) at Fermi level.

Table 1
Variations of E_σ; (eV) and σ'_o (Ω^{-1} cm^{-1} K) with Ag content for the $Ag_x(As_{0.4}Se_{0.6})_{100\_x}$ compositions

x (at.%)	5	7.5	10	12.5	15	17.5
E_σ (eV)	0.276	0.265	0.263	0.258	0.247	0.246
σ'_o (Ω^{-1} Cm^{-1} K)	0.036	0.065	0.173	0.342	0.360	1.066

Fig. 8 shows the linear fitting of σ-T data in temperature range $T \leq 223$ K according to Mott's relation (Eq. (3)) for Ag_x $(As_{0.4}Se_{0.6})$ $_{100\_x}$ compositions. The slopes of data in Fig. 8 are used to calculate Mott's parameters of variable range hopping conduction. The density of localized states (DOLS) at Fermi level $N(E_F)$ can be used to calculate the hopping distance (R_{av}) and hopping energy (W). In Mott's theory R_{av} and W are given by:

$$R_{av} = \left[\frac{9}{8\pi\alpha N(E_F)k_B T}\right]^{1/4} \tag{5}$$

$$W = \frac{3}{4\pi R_{av}^3 N(E_F)} = \left[\frac{2\alpha^3 k_B^3 T^3}{9\pi N(E_F)}\right]^{1/4} \tag{6}$$

The concentration of conduction electrons (N) within a range of k_B T of the Fermi energy can be calculated from $2k_B$ T N (E_F) [19]. The compositional dependencies of $N(E_F)$, N, R_{av} and W for $Ag_x(As_{0.4}Se_{0.6})_{100\_x}$ compositions are calculated and recorded in Table 2.

The obtained $N(E_F)$ and N data are unsequentially changed with x for the investigated compositions. The values of N (E_F) and N have a maximum at lowest concentration of silver and both R_{av} and W have a maximum at $x = 15$ at%, while the former parameters have a minimum values at $x = 5$ at%, and the latter ones have a maximum values at $x = 15$ at%. On the other side, the values of σ''_o are increased with increasing Ag content except at higher Ag concentration, it was decreased. These values, however, are relatively high compared to those recorded previously [6] for some chalcogenide glasses. The small values of both R and W which are approximately satisfying the conditions of Mott's VRH process; $\alpha R_{av} \gg 1$ and $W > k_B T$, can be attributed to the obtained unreasonably high values of N (E_F). The disparities in N (E_F) evaluation are also observed for some semiconducting materials [20] and have been attributed to the incorrect assumptions of Mott's

Table 2
Variations of $N(E_F)$ ($cm^{-3}\,eV^{-1}$), N (cm^{-3}), R_{av} (Å), W (eV) and σ_o'' ($\Omega^{-1}\,cm^{-1}\,K^{1/2}$) as functions of compositions for $Ag_x(As_{0.4}Se_{0.6})_{100\_x}$ chalcogenide system

x (at. %)	$N(E_F)$ ($cm^{-3}\,eV^{-1}$)	N (cm^{-3})	R_{av} (Å)	W (eV)	σ_o'' ($\Omega^{-1}\,cm^{-1}\,K^{1/2}$)
5	2.3×10^{20}	12×10^{18}	27.73	47.78×10^{-3}	0.0046×10^{-5}
7.5	1.0×10^{20}	5.3×10^{18}	34.04	58.65×10^{-3}	0.0470×10^{-5}
10	1.7×10^{20}	8.7×10^{18}	30.13	51.92×10^{-3}	0.0530×10^{-5}
12.5	0.64×10^{20}	3.3×10^{18}	38.31	66.00×10^{-3}	10.300×10^{-5}
15	0.35×10^{20}	1.8×10^{18}	44.54	76.75×10^{-3}	135.50×10^{-5}
17.5	0.44×10^{20}	2.3×10^{18}	42.15	72.63×10^{-3}	103.40×10^{-5}

derivation of a VRH relations, such as the energy independence of the density of localized state at Fermi level, neglection of the correlation effect in tunneling process and neglection of electron-phonon interaction.

Fig. 9 shows the plots of Seebeck coefficient S versus the reciprocal temperature for the six mentioned compositions. As it is seen in this figure, within the whole temperature considered for measurements $253 \le T \le 373$ K, the generated thermoelectric power (TEP) possessed positive sign similar to typical p-type semiconductors. Such positive Seebeck values confirm that the contribution to the observed TEP is mainly due to holes and/or positive ions (Ag^+). Accordingly [12] the Ag^+ ionic conductivity is larger than the electronic conductivity. These holes and positive ions contribution are thermally activated. The continuous increase of positive sign Seebeck coefficient emphasizes continuous domination of the thermally activated holes and/or Ag^+ ions contribution to the observed thermoelectric power. Linear plots shown in Fig. 9 indicate that the temperature dependence of Seebeck coefficient can be described by the following equation [20]:

$$S = \pm\frac{k_B}{e}\left(\frac{E_s}{k_B T} + A\right) \tag{7}$$

where e is the electron charge and A is a dimensionless parameter which concerns the carrier scattering mechanism [15] or assumed to be a measure of the kinetic energy transported by carries [21]. The plus sign holds for the p-type and minus sign holds for n-type semiconductors, respectively. As already mentioned, S possessed positive sign for all the investigated compositions and within the whole range considered for temperature.

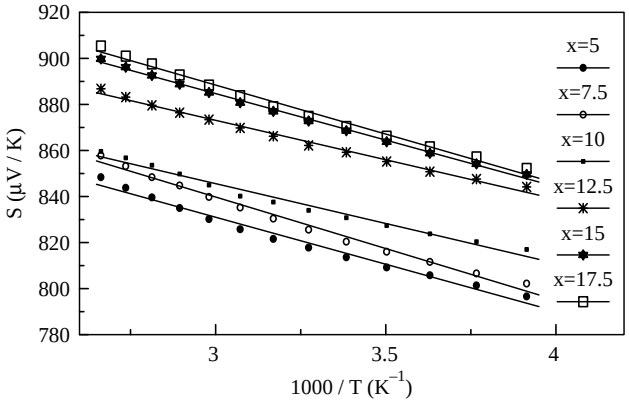

Fig. 9. The temperature dependence of Seebeck coefficient for $Ag_x(As_{0.4}Se_{0.6})_{100\_x}$ compositions.

Slope of all S versus $1/T$ plots possessed minus sign confirming an increase of holes and Ag^+ ions contribution with increasing T which confirms in turn that, transition of material to n-type with dominant activation of electrons is unexpected at higher temperatures. Therefore, applying the above equation, permit us to calculate both the electrochemical potential E_s and dimensionless parameter A which are recorded in Table 3. It is seen from Table 3 that values of E_s are increased with increasing Ag content. This may be attributed to the increase of Ag^+ ions, which in turn resulted from the increase in silver content. On the other hand, the parameter A possessed anomalously high values, which are unusual for normal semiconductors. However, this observation may be attributed to the relatively higher effective mass of Ag ions compared to those of holes.

The recorded data of E_σ and E_s which are listes in Tables 1 and 3, respectively reveal that $E_\sigma > E_s$. Accordingly to [22,23], three different models have been proposed to explain the inconsistency in the values of E_σ and E_s. These are:

(i) two-carriers conduction,
(ii) one-carrier conduction with thermally activated mobility and
(iii) a two-channel conduction model where the conduction occurs through both the extended states and hopping through the tail of localized states. For the present system, the variation in σ with the ambient temperature indicates that the third model can be used to explain the obtained results.

Table 3
Variations of activation energy of Seebeck coefficient E_s (μ eV) and the parameter A for $Ag_x(As_{0.4}Se_{0.6})_{100\_x}$ compositions

Parameter	Ag content					
	5	7.5	10	12.5	15	17.5
E_s(μ eV)	36.789	37.753	38.968	39.557	40.420	41.612
A	939.26	949.00	962.17	991.4	1006.0	1013.0

4. Conclusion

The X-ray diffraction investigations confirmed the polycrystalline nature for $Ag_x (As_{0.4}Se_{0.6})_{100\_x}$ chalcogenide compositions prepared with $5 \leq x \leq 10$ at% and amorphous structure for compositions prepared with $125 \leq x \leq 17.5$ at%. From the d.c. conductivity measurements it can be extracted that:

(i) At certain ambient temperature, values of σ were increased with increasing Ag content.
(ii) The conduction phenomena of the present alloys have emerge through two mechanisms. The thermally activated conduction through the extended states, which dominates in the relatively higher temperature range $T > 223$ K and the hopping conduction through the localized states appearing at relatively lower temperatures range ($T \leq 223$ K).
(iii) The activation energy of electrical conductivity (E_σ) was found to decrease with increasing Ag content.
(iv) The values of $N(E_F)$, N, R_{av} and W were estimated. Values of $N(E_F)$ were found to be unreasonably high compared with those established for some glasses of Ag–As–Se system. Such disparities in $N(E_F)$ were attributed to the numerous simplifying assumptions used in derivation of Mott's equation.

Finally, the values of the generated thermoelectric power (Seebeck coefficient) of the investigated glasses are positive in sign. Besides, their values at ambient temperature increased with increasing Ag content. This behaviour can be attributed to the increase of Ag^+ ion concentration.

Acknowledgements

The authors are grateful to Mr. H. F. Mohamed for his valuable experimental assistance.

References

[1] G. Luckovsky, F.L. Geleener, R.H. Geils, R.C. Keezer, in: P.H. Gaskell (Ed.), The structure of Non-Crystalline Materials, Taylor and Francis, London, 1977, p. 127.
[2] M.M. Wakkad, E.Kh. Shokr, S.H. Mohamed, Phys. Stat. Sol. (a) 183 (2) (2001) 399.
[3] M.M. Wakkad, E.Kh. Shokr, S.H. Mohamed, J. Non-Cryst. Solids 265 (2000) 157.
[4] M.M. Wakkad, J. Thermal Anal. Calor. 63 (2001) 533.
[5] M.M. AbdEL-Raheem, M.M. Wakkad, N.M. Megahed, A.M. Ahmed, E.Kh. Shokr, M. Dongol, J. Mater. Sci. 31 (1996) 5759.
[6] P.S.L. Narasimham, A. Giridhar, S. Mahadevan, J. Non-Cryst. Solids 43 (1981) 365.
[7] M. Itoh, J. Non-Cryst Solids 210 (1997) 178.
[8] C.J. Benmore, P.S. Salmon, Phys. Rev. Lett. 73 (1994) 264.
[9] V. Mastelaro, S. Benazeth, H. Dexpert, J. Non-Cryst Solid 185 (1995) 274.
[10] A.L. Laskar, S. Chandra, Superionic Solids And Solid Electrolytes: Recent Trends, Academic Press, London, 1989.
[11] T. Takahashi, High Counductivity Solid State Conductors-Recent Trends And Applications, World Scientific, Singapore, 1989.
[12] A. Karthikeyan, Satyanarayana, J. Power Sources 51 (1994) 457.
[13] S.R. Elliot, Nature 354 (1991) 445.
[14] S.R. Elliot, Physics of Amorphous Materials, 2nd ed., Essex, Longman, 1990. p. 71.
[15] M. Ohto, K. Tanaka, J. Non-Cryst Solids 227 (1998) 784.
[16] H. Naito, Y. Kanemitsu, Phys. Rev. B 49 (1994) 10131.
[17] N.F. Mott, E.A. Davis, Electronic press in Non-Crystalline Materials, Clarendon Press, Oxford, 1979.
[18] H. Fritzsche, in: J. Tauc (Ed.), Amorphous and Liquid Semiconductors, Plenum Press, London, 1974, p. 221.
[19] P. Nagels, E. Sleeckx, R. Callaerts, L. Tichy, Solid State Commun. 94 (1993) 49.
[20] D. Lemoine, J. Mendolia, Phys. Lett. A. 22 (1981) 418.
[21] J. Tauc, Photo and thermoelectric effects in semiconductors, Pergamon, New York, 1962.
[22] N. Tohge, T. Minami, M. Tanaka, J. Non-Cryst Solids 37 (1980) 23.
[23] N.F. Mott, E.A. Davis, R.A. Street, Phil. Mag. 32 (1975) 961.